International Journal of Mechanical Engineering and Technology (IJMET)
Volume 9, Issue 8, August 2018, pp. 712–721, Article ID: IJMET_09_08_076
Available online at http://www.iaeme.com/ijmet/issues.asp?JType=IJMET&VType=9&IType=8
ISSN Print: 0976-6340 and ISSN Online: 0976-6359

ANALYSIS OF HALL EFFECTS ON THE ENTROPY GENERATION OF NATURAL CONVECTION FLOW THROUGH A VERTICAL MICROCHANNEL

O. O. Agboola, A. A. Opanuga, Hilary I. Okagbue, S. A. Bishop, P. O. Ogunniyi
Department of Mathematics, Covenant University, Ota, Ogun State, Nigeria

ABSTRACT

In this work, the entropy generation of a steady fully developed natural convection flow between two vertical parallel microchannels with Hall effect is investigated. The effects of velocity slip and temperature jump at the solid-fluid interface are considered. The differential equations obtained from the derived governing equations are transformed and the solutions of the velocity and temperature profiles are constructed via differential transform method. Plots are presented to explain the influence of Hall current, Wall-ambient temperature difference ratio and fluid wall interaction parameter effects on fluid motion, fluid temperature, fluid irreversibility and Bejan number. The results indicate that both Hall current and Wall-ambient temperature difference ratio (WATDR) encourage fluid irreversibility whereas fluid wall interaction parameter (FWIP) reduces fluid irreversibility.

Keywords: Hall current, Microchannel flow, Natural convection, Entropy generation and Differential transform method.
Cite this Article: O. O. Agboola, A. A. Opanuga, Hilary I. Okagbue, S. A. Bishop and P. O. Ogunniyi, Analysis of Hall Effects on the Entropy Generation of Natural Convection flow Through a Vertical Microchannel, International Journal of Mechanical Engineering and Technology, 9(8), 2018, pp. 712–721.
http://www.iaeme.com/IJMET/issues.asp?JType=IJMET&VType=9&IType=8

1. INTRODUCTION

In recent times, studies of microchannels flows have received a boost due to the evolution of advanced techniques in manufacturing processes, which has led to the reduction in the size of various industrial and engineering designs. Applications are found in areas such as medical and biomedical use, computer chips and chemical separations. It is used in the cooling of electronic devices, micro air vehicles (MAV), micro heat exchanger systems, micro-channel heat sink, microjet impingement cooling, micro heat pipe and aircraft intake de-icing. The Knudsen number is the fundamental quantity in micro-channel analysis; it is defined as the

ratio of molecular mean free path to the characteristic length. Schaaf and Chambre [1] in their work gave a classification of different flow regimes based on Knudsen number.

Numerous investigations have been undertaken to improve design of fluid flow and heat transfer in microchannel. Exact solution of fully developed natural convection in an open-ended vertical parallel-plate microchannel with asymmetric wall temperature distributions was obtained by Chen and Weng [2]. It was indicated that rarefaction and fluid-wall interaction enhanced the volume flow rate but decreased heat transfer rate. Moreover, it was also observed that microscale volume flow rate is higher than macroscale volume flow rate. This work was further extended by Jha et al. [3] with the inclusion of suction/injection effect. Their results showed that skin-friction and heat transfer depend strongly on suction/injection parameter. Adesanya [4] analysed the effects of velocity slip and temperature jump on free convective flow of heat generating fluid through a porous vertical channel. It was concluded that an increase in the slip parameter enhanced the flow of fluid and decreased the shear stress at the suction wall. Moreover, fluid temperature rose higher while the rate of heat transfer at the suction wall decreased with an increase in the temperature jump parameter. Weng and Cheng [5] analysed natural convection flow with the effects of variable thermal-physical properties in a vertical parallel-plate microchannel. It was submitted that velocity slip and temperature jump for an air flow increased with increase in variable properties effect. Khadrawi et al. [6] investigated the transient hydrodynamics and thermal behavior of fluid flow in an open-ended vertical parallel plate microchannel. It was shown that increase in Knudsen number the increases slip in the hydrodynamics and thermal boundary condition. Recently, Jha and his associates carried out extensive investigation on this subject matter in [7-9].

Over the past decades scientists and engineers have established the fact that entropy generation which destroys available energy exists due to heat transfer at different modes in thermal designs. Recent findings have shown that first law of thermodynamics has proved inadequate in monitoring irreversibility associated with thermal designs. However, second law analysis introduced by Bejan [10-11] has gained wide applications due to its robustness and accuracy. This approach has subsequently been applied by various investigators to further establish other factors contributing to loss of useful energy. Few of these are Adesanya et al. [12-14], Adesanya and Makinde [15-16], Ajibade and Jha [17], Eegunjobi and Makinde [18-19], Das and Jana [20] and recently Opanuga et al. [21-24]. This approach is applied in this investigation to monitor possible loss of exergy in microchannel flows. This became necessary owing to the fact that more heat is dissipated as the sizes of electronic devices reduce as in microchannel flow designs.

In this work, entropy generation in microchannel flow with Hall effect is analysed. The velocity and temperature profiles are solved using the semi-analytical technique introduced by Zhou [25] and adopted by many other researchers to tackle various linear and nonlinear models [26-30].

2. PROBLEM FORMULATION

Consider a vertical microchannel of fully developed incompressible and electrically conducting natural convection flow of viscous fluid formed by two infinite vertical parallel plates. Relatively high electron-atom collision frequency assumption is taken so that the influence of Hall current is upheld. Effects of velocity slip and temperature jump are taken into account, furthermore induced magnetic field effect arising due to the motion of an electrically conducting fluid is taken into consideration. There is an asymmetric heating of the plates such that the hotter plate ($y = 0$) is maintained at temperature T_1 while the cooler plate (

$y = h$) is at temperature T_2 and $T_1 > T_2$ Following Jha et al. [8] and under Boussinesq's approximation, the governing equations are:

$$\rho\nu_{\circ}\frac{du^*}{dy^*} = \mu\frac{d^2u^*}{dy^{*2}} + g\beta\left(T_1 - T_0\right) - \frac{\sigma B_0^2}{1+m^2}\left(u^* - mw^*\right); \quad (1)$$

$$\rho\nu_{\circ}\frac{dw^*}{dy^*} = \mu\frac{d^2w^*}{dy^{*2}} - \frac{\sigma B_0^2}{1+m^2}\left(w^* + mu^*\right); \quad (2)$$

$$\rho c_p\frac{dT^*}{dy^*} = k\frac{d^2T^*}{dy^{*2}} + \mu\left[\left(\frac{du^*}{dy^*}\right)^2 + \left(\frac{dw^*}{dy^*}\right)^2\right] + \frac{\sigma B_0^2}{1+m^2}\left(w^{*2} + u^{*^2}\right); \quad (3)$$

with the following boundary conditions

$$u = \frac{2-f_v}{f_v}\lambda\frac{du}{dy}, \quad w = \frac{2-f_v}{f_v}\lambda\frac{dw}{dy}, \quad T = T_2, + \frac{2-f_t}{f_t}\frac{2\gamma}{\gamma+1}\frac{\lambda}{\mathrm{Pr}}\frac{dT}{dy}, \quad y = 0,$$
$$u = -\frac{2-f_v}{f_v}\lambda\frac{du}{dy}, \quad w = -\frac{2-f_v}{f_v}\lambda\frac{dw}{dy}, \quad T = T_1 - \frac{2-f_t}{f_t}\frac{2\gamma}{\gamma+1}\frac{\lambda}{\mathrm{Pr}}\frac{dT}{dy}, \quad y = h \quad (4)$$

Introducing the non-dimensional expressions

$$y = \frac{y^*}{h},\ u = \frac{u^*}{v_0}, w = \frac{w^*}{v_0},\ \theta = \frac{T^* - T_0}{T_1 - T_0},\ s = \frac{v_0 h}{\nu}, \nu = \frac{\mu}{\rho},\ H^2 = \frac{\sigma B_0^2 h^2}{\mu}, kn = \frac{\lambda}{b},$$
$$\Omega = \frac{T_1 - T_0}{T_0},\ Br = \frac{\mu v_0^2}{k\left(T_1 - T_0\right)},\ \mathrm{Pr} = \frac{\nu\rho c_p}{k},\ Ns = \frac{T_0^2 h^2 E_G}{k(T_1 - T_0)^2}, Gr = \frac{g\beta h^2(T_1 - T_0)}{\mu\nu},$$
$$\xi\left(T_2 - T_0\right) = T_1 - T_0,\ \beta_v = \frac{2-F_v}{F_v},\ \beta_t = \frac{2-F_v}{F_v}\frac{2\gamma_s}{\gamma_s+1}\frac{1}{\mathrm{Pr}},\ \gamma_s = \frac{c_p}{c_v}, \ln = \frac{\beta_t}{\beta_v} \quad (5)$$

Equations (1)-(3) yield

$$\mathrm{Re}\frac{du}{dy} = \frac{d^2u}{dy^2} + Gr\theta - \frac{M^2}{1+m^2}(u - mw); \quad (6)$$

$$\mathrm{Re}\frac{dw}{dy} = \frac{d^2w}{dy^2} - \frac{M^2}{1+m^2}\left(w + mu\right), \quad (7)$$

$$\mathrm{Re}\,p_r\frac{d\theta}{dy} = \frac{d^2\theta}{dy^2} + Br\left[\left(\frac{du}{dy}\right)^2 + \left(\frac{dw}{dy}\right)^2\right] + \frac{BrM^2}{1+m^2}\left(w^2 + u^2\right), \quad (8)$$

The dimensionless boundary conditions are obtained as

$$u = \beta_v kn\frac{du}{dy}, \quad w = \beta_v kn\frac{dw}{dy}, \quad \theta = \xi + \beta_v knln\frac{d\theta}{dy}, \quad y = 0,$$
$$u = -\beta_v kn\frac{du}{dy}, \quad w = -\beta_v kn\frac{dw}{dy}, \quad \theta = 1 - \beta_v knln\frac{d\theta}{dy}, \quad y = 1 \quad (9)$$

Table 1 Operations and Properties of Differential Transform Method

Original function	Transformed function
$f(y)=u(y)\pm w(y)$	$F(k)=U(k)\pm W(k)$
$f(y)=\frac{d^n u(y)}{dy^n}$	$F(k)=\frac{(k+n)!}{k!}U(k+n)$
$f(y)=u^2$	$F(k)=\sum_{r=0}^{k}U(r)U(k-r)$
$f(y)=\left(\frac{du(y)}{dy}\right)^2$	$F(k)=\sum_{r=0}^{k}(r+1)(k-r+1)U(r+1)U(k-r+1)$
$f(y)=\left(\frac{d^2u(y)}{dy^2}\right)^2$	$F(k)=\sum_{r=0}^{k}(r+1)(r+2)(k-r+1)(k-r+2)U(r+2)U(k-r+2)$

3. DIFFERENTIAL TRANSFORM METHOD OF SOLUTION

The basic operations of differential transform method (DTM) used in this paper are summarized in Table 1. (See [26-30]. By applying appropriate operations from Table 1 to transform equations (5)-(7), one obtains the following recurrence relations:

$$U(k+2)=\frac{1}{(k+1)(k+2)}\left[\mathrm{Re}(k+1)U(k+1)-Gr\Theta(k)+\frac{M^2}{1+m^2}(U(k)-mW(k))\right] \quad 10$$

$$W(k+2)=\frac{1}{(k+1)(k+2)}\left[\mathrm{Re}(k+1)W(k+1)+\frac{M^2}{1+m^2}(W(k)+mU(k))\right] \quad 11$$

$$\begin{aligned}\Theta(k+2)=\frac{1}{(k+1)(k+2)}\Bigg[&\mathrm{Re}\,\mathrm{Pr}(k+1)\Theta(k+1)-Br\left(\sum_{r=0}^{k}(r+1)(k-r+1)U(k-r+1)\right.\\&\left.+\sum_{r=0}^{k}(r+1)(k-r+1)W(k-r+1)\right)\\&-\frac{BrM^2}{1+m^2}\left(\sum_{r=0}^{k}F(r)U(k-r)+\sum_{r=0}^{k}W(r)U(k-r)\right)\Bigg]\end{aligned} \quad 12$$

where $U(k)$, $W(k)$ and $\Theta(k)$ are the DTM transformed forms of the functions $u(y)$, $w(y)$ and $\theta(y)$ respectively. From the principle of DTM, the functions $u(y)$, $w(y)$ and $\theta(y)$ can be written in terms of $U(k)$, $W(y)$, $\Theta(k)$ as

$$u(y)=\sum_{k=0}^{n}y^kU(k),\ w(y)=\sum_{k=0}^{n}y^kW(k),\ \theta(y)=\sum_{k=0}^{n}y^k\Theta(k), \quad 13$$

where n, being the size of each series is determined upon the convergence of the series.

Using the recursive relations (9)-(11), one can obtain the values of the coefficients $U(j)$, $W(j)$ and $\Theta(j)$ for $j\geq 4$ by setting $k=0,1,2,\ldots$ With the values of these coefficients, the series solutions $u(y)$, $w(y)$ and $\theta(y)$ are then obtained using equations (12) (in terms of $U(k)$, $W(k)$ and $\Theta(k)$) for $k=0,1$. Next, the boundary conditions in (8) are invoked on the

series solutions $u(y)$, $w(y)$ and $\theta(y)$ to generate a system of six equations in six unknowns, that is, $U(0)$, $U(1)$, $W(0)$, $W(1)$, $\Theta(0)$ and $\Theta(1)$. The values of these unknowns can be obtained readily by solving the system of equations. Finally, the series solutions for $u(y)$, $w(y)$ and $\theta(y)$ can be obtained.

To achieve this, appropriate coding was carried out in Maple environment. Coding equations (10-13) in symbolic Maple software yields the approximate solution. The results are presented in Figures 1-4.

4. ENTROPY GENERATION ANALYSIS

The local entropy generation for the flow is given as Bejan [11]:

$$E_G = \frac{k}{T_0^2}\left(\frac{dT^*}{dy^*}\right)^2 + \frac{\mu}{T_0}\left(\left(\frac{du^*}{dy^*}\right)^2 + \left(\frac{dw^*}{dy^*}\right)^2\right) + \frac{\sigma B_0^2}{T_0}\left(w^{*2} + u^{*2}\right), \tag{14}$$

The first term on the right-hand side of equation (14) is entropy generation due to heat transfer, the second term represents entropy generation due to viscous dissipation and the last term is entropy generation due to the effect of magnetic field.

and 0.042 kg/s. Figure 3 shows the variation in wind speed for these days.

Using (4) in equation (14) the dimensionless form of entropy generation is written as:

$$Ns = \left(\frac{d\theta}{dy}\right)^2 + \frac{Br}{\Omega}\left(\left(\frac{du}{dy}\right)^2 + \left(\frac{dw}{dy}\right)^2\right) + \frac{BrM^2}{\Omega}\left(w^2 + u^2\right), \tag{15}$$

where E_G and N_s are the dimensional and dimensionless entropy generation rate, respectively. The ratio of heat transfer entropy generation (N_1) to fluid friction entropy generation (N_2) is represented as

$$\Phi = \frac{N_2}{N_1} \tag{16}$$

Alternatively, Bejan number gives the entropy generation distribution ratio parameter; it represents the ratio of heat transfer entropy generation to the total entropy generation due to heat transfer and fluid friction, which is defined as

$$Be = \frac{N_1}{N_s} = \frac{1}{1+\Phi} \tag{17}$$

and

$$Be = \begin{cases} 0, N_2 \square N_1 \\ 0.5, N_1 = N_2 \\ 1, N_2 \square N_1 \end{cases} \tag{18}$$

5. DISCUSSION OF RESULTS

To discuss the influence of Hall parameter (m), fluid wall interaction parameter (FWIP) $(\ln)$ and wall-ambient temperature difference ratio (WATDR) (ξ) on the flow, the plots for primary velocity, secondary velocity, entropy generation and irreversibility ratio are presented

in Figures 1-4 while by fixing the parameters $Br = 1, \Pr = 0.71$, $\mathrm{Re} = 2, \beta_v kn = 0.05$, $\ln = 1.667, \Omega = 1, Gr = 1$. The values chosen for $\beta vkn = 0.05$ (which depicts a measure of the departure from the continuum regime) and $\ln = 1.667$ (fluid wall interaction parameter) are from Cheng and Weng [2].

5.1. Influence of Hall current parameter

Figures 1 and 2 depict the effect of Hall parameter on fluid velocity. It is evident that the fluid velocity is enhanced as Hall parameter increases. This is as a result of the reduction in the resistive influence of the magnetic field on fluid motion as Hall parameter increases. In Figure 3, entropy generation is shown to increase slightly as Hall parameter increases. It is surprising that Hall parameter does not have much impact on entropy generation. Furthermore, in Figure 4, Bejan number is reduced as Hall current increases. This reveals that fluid friction irreversibility dominate over heat transfer irreversibility as Hall effect becomes more pronounced.

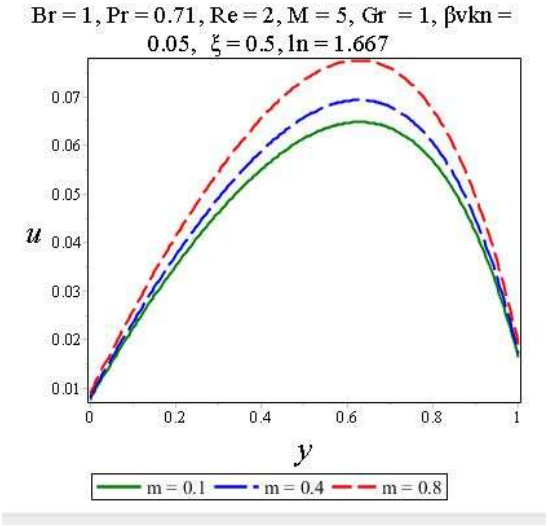

Figure 1 Hall Current Vs Primary Velocity

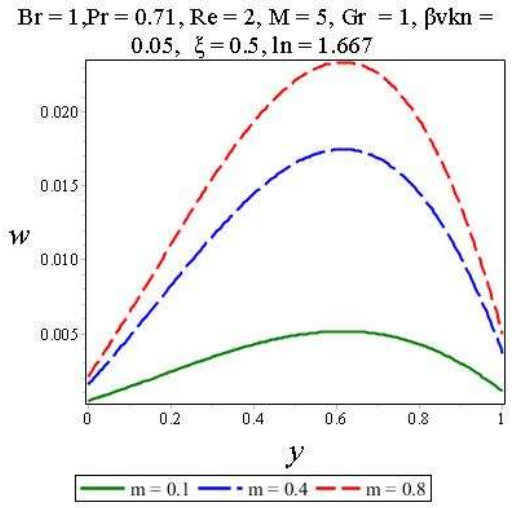

Figure 2 Hall Current Vs Secondary Velocity

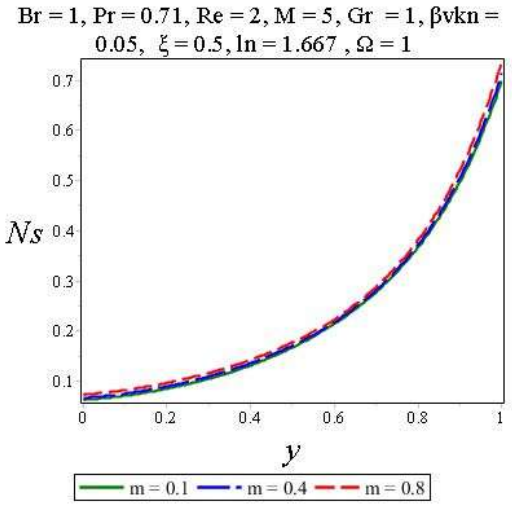

Figure 3 Hall Current Vs Entropy Generations

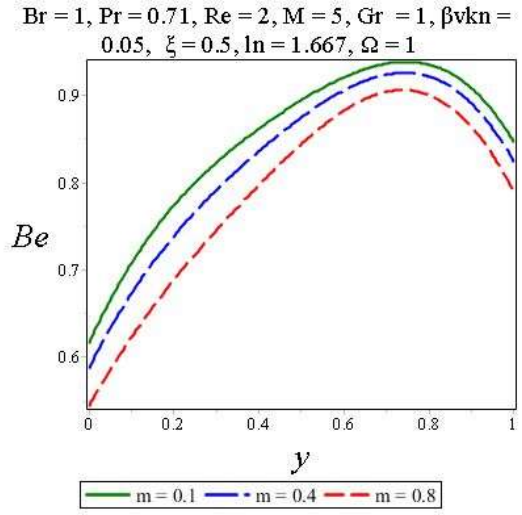

Figure 4 Hall Current Vs Bejan Number

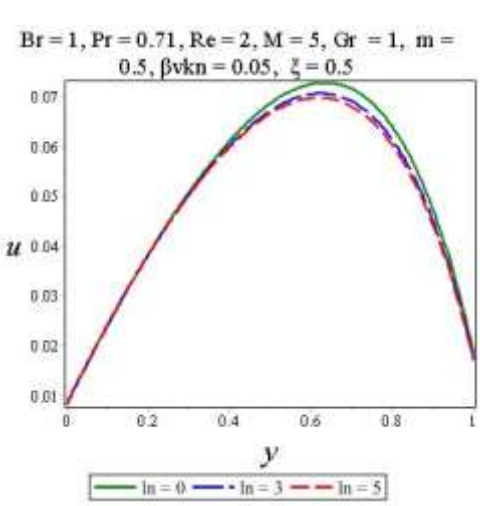

Figure 5 FWIP Vs Primary Velocity

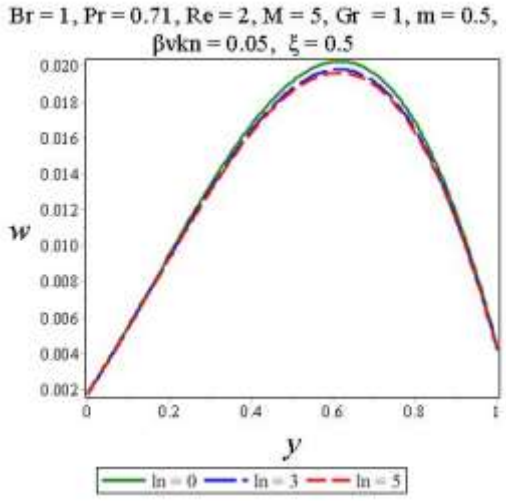

Figure 6 FWIP Vs Secondary Velocity

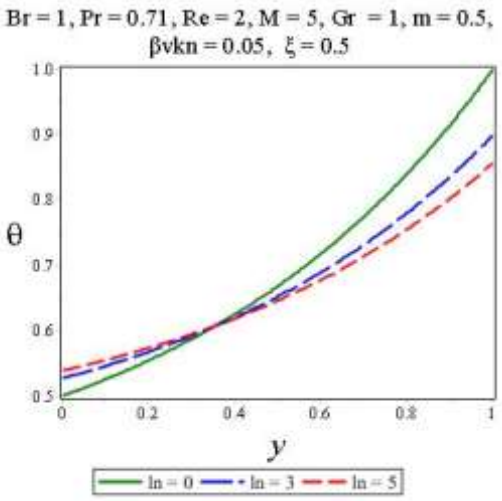

Figure 7 FWIP Vs Temperature

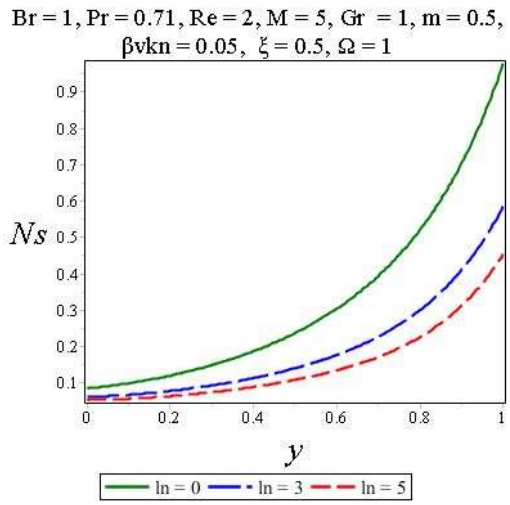

Figure 8 FWIP Vs Entropy Generations

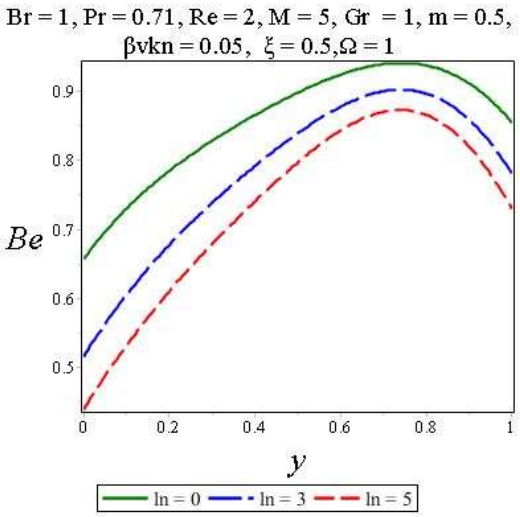

Figure 9 FWIP Vs Bejan Number

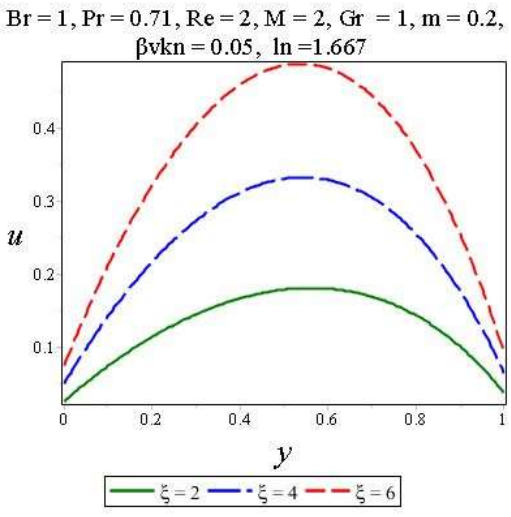

Figure 10 WATDR Vs Primary Velocity

5.2. Influence of fluid- wall interaction parameter (FWIP)

Figures 5 and 6 present the effect of FWIP $(\ln)$ on fluid velocity. As FWIP increases it is interesting to note that both primary and secondary velocity are found to be retarded in the middle of the microchannel. In Figure 7, fluid temperature is found to have risen in the region $0 \le y \le 0.35$ while it experiences a sharp decline around $0.35 \le y \le 1$. The effect of this observation is noted in Figure 8 which represents the influence of FWIP on the entropy generation of the fluid. It is clearly shown that fluid entropy generation is completely retarded as FWIP increases. In Figure 9 Bejan number declines with a rise in FWIP indicating that fluid irreversibility is as a result of viscous dissipation.

5.3. Influence of wall-ambient temperature difference ratio (WATDR) (ξ)

Figures 10 and 11 represent the variation effect of wall-ambient temperature difference ratio WATDR (ξ) both primary and secondary velocity. There is a rise in both primary and secondary velocity as WATDR increases in values. Next is the effect of WATDR on fluid temperature, it is noted that fluid temperature rises significantly with increase in WATDR as shown in Figure 12. The rise in temperature has a considerable influence on the entropy generation as depicted in Figure 13. It is clearly seen that fluid irreversibility receives a boost as the value of WATDR varies. In Figure 14 fluid entropy generation as a result of the varying values of WATDR is shown to have been occasioned by heat transfer irreversibility since Bejan number increases in values with increase in WATDR.

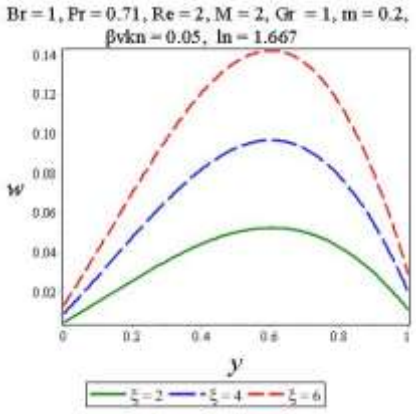

Figure 11 WATDR Vs Secondary Velocity

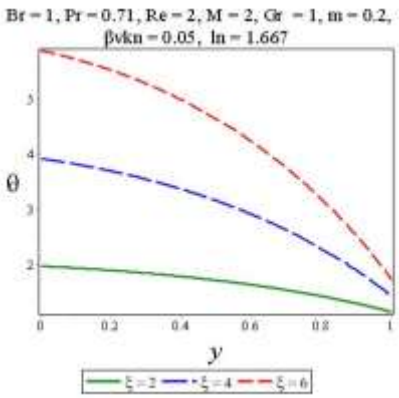

Figure 12 WATDR Vs Temperature

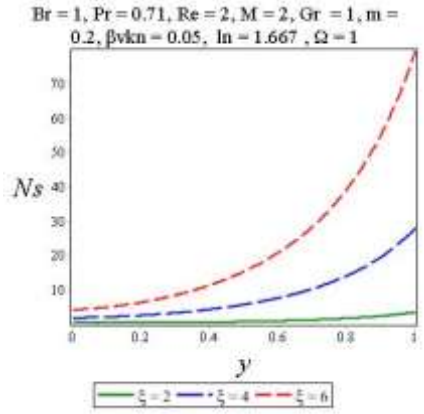

Figure 13 WATDR Vs Entropy Generation

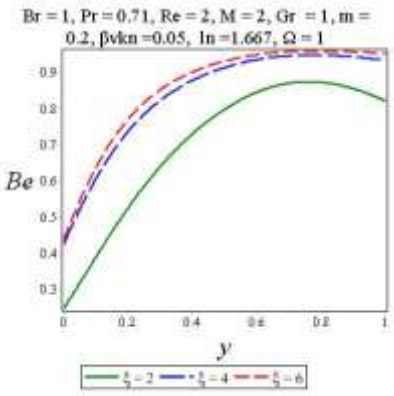

Figure 14 WATDR Vs Bejan Number

6. CONCLUSION

In this work, a mathematical model has been formulated to investigate the influence of Hall current on the entropy generation of hydromagnetic natural convection microchannel flow between two infinite vertical parallel plates under the influence of velocity slip and temperature jump parameters conditions. The velocity and temperature profiles obtained from the governing equations are solved via differential transform technique and the results are substituted into the expression for the entropy generation and Bejan number. The main contributions of this article are as follows:

1. Hall current enhance fluid motion and entropy generation,
2. Fluid wall interaction parameter (FWIP) impedes fluid velocity and reduces entropy generation,
3. Wall-ambient temperature difference ratio (WATDR) increases both primary and secondary velocity and entropy generation,
4. Fluid entropy generation is contributed by both fluid friction and heat transfer irreversibility

REFERENCES

[1] Schaaf, S. A. and Chambre, P. L. Flow of Rarefied Gases. Princeton: Princeton University Press, 1961.

[2] Chen, C. K. and Weng, H. C. Natural convection in a vertical microchannel. J. Heat Transfer, 127, 2005, pp. 1053–1056.

[3] Jha, B. K, Aina, B. and Joseph, S. B. Natural convection flow in vertical micro-channel with Suction/Injection, J. Process Mech. Eng., 228 (3) , 2014, pp. 171–180.

[4] Adesanya, S. O. Free convective flow of heat generating fluid through a porous vertical channel with velocity slip and temperature jump. Ain Shams Eng J, 2015, http://dx.doi.org/10.1016/j.asej.2014.12.008

[5] Weng, H. C. and Chen, C. K. Variable physical properties in natural convective gas microflow. J. Heat Transf., 130, 2008, 082401.

[6] Khadrawi, A. F., Othman, A. and Al-Nimr, M. A. Transient free convection fluid flow in a vertical microchannel as described by the hyperbolic heat conduction model. Int. J. Thermophys., 26(3), 2005, pp. 905–918.

[7] Jha, B. K., Aina, B. and Ajiya, A. T. MHD natural convection flow in a vertical parallel plate microchannel, Ain Shams Engineering Journal, 6, 2015, pp. 289–295.

[8] B.K. Jha et al., Hall effects on MHD natural convection flow in a vertical microchannel, Alexandria Eng. J. (2017), http://dx.doi.org/10.1016/j.aej.2017.01.038

[9] Jha, B. K., Aina, B. and Sani, I. Transient magnetohydrodynamic free convective flow in vertical microconcentric-annuli, Proc. IMechE Part N: J. Nanoeng. Nanosyst., (2015), http://dx.doi.org/10.1177/1740349915578956.

[10] Bejan, A. A study of entropy generation in fundamental convective heat transfer. ASME J. Heat Transf., 101, 1979, pp. 718–725.

[11] Bejan, A. Second law analysis in heat transfer and thermal design. Adv. Heat Transf. 15, 1982, pp. 1–58.

[12] Adesanya, S. O., Falade, J. A., Jangili, S. and Beg, O. A. Irreversibility analysis for reactive third-grade fluid flow and heat transfer with convective wall cooling. Alexandria Engineering Journal, 56, 2017, pp. 153–160.

[13] Adesanya, S. O., Kareem, S.O., Falade, J. A. and Arekete, S. A. Entropy generation analysis for a reactive couple stress fluid flow through a channel saturated with porous material. Energy, 93, 2015, pp. 1239-1245.

[14] Jangili, S., Adesanya, S. O., Falade, J. A. and Gajjela, N. Entropy generation analysis for a radiative micropolar lluid flow through a vertical channel saturated with non-darcian porous medium. Int. J. Appl. Comput. Math. DOI 10.1007/s40819-017-0322-8

[15] Adesanya, S. O. and Makinde, O. D. Irreversibility analysis in a couple stress film flow along an inclined heated plate with adiabatic free surface. Physica A, 432, 2015, pp. 222–229.

[16] Adesanya, S. O. and Makinde, O. D. Effects of couple stresses on entropy generation rate in a porous channel with convective heating. Comp. Appl. Math., 34, 2015, pp. 293–307. DOI 10.1007/s40314-014-0117-z

[17] Ajibade, A. O., Jha, B K. and Omame, A. Entropy generation under the effect of suction/injection. Applied Mathematical Modelling, 35, 2011, pp. 4630–4646.

[18] Eegunjobi, A. S. and Makinde, O. D. Effects of navier slip on entropy generation in a porous channel with suction/injection. Journal of Thermal Science and Technology, 7(4), 2012, pp. 522-535.

[19] Eegunjobi, A. S. and Makinde, O. D. Combined effect of buoyancy force and navier slip on entropy generation in a vertical porous channel. Entropy, 14, 2012, pp. 1028-1044, doi:10.3390/e14061028.

[20] Das, S. and Jana, R. N. Entropy generation due to MHD flow in a porous channel with Navier slip. Ain Shams Engineering Journal, 5, 2014, pp. 575–584.

[21] Opanuga, A. A., Gbadeyan, J. A., Iyase, S. A. and Okagbue, H. I. Effect of thermal radiation on the entropy generation of hydromagnetic flow through porous channel. The Pacific Journal of Science and Technology, 17(2), 2016, pp. 59-68.

[22] Opanuga, A. A., Okagbue, H. I., Agboola, O. O. and Imaga, O. F. Entropy Generation analysis of buoyancy effect on Hydromagnetic poiseuille flow with internal heat generation. Defect and Diffusion Forum, 378, 2017, pp. 102-112.

[23] Opanuga, A. A., Gbadeyan, J. A. and Iyase, S. A. Second law analysis of Hydromagnetic couple stress fluid embedded in a non-Darcian porous medium. IAENG International Journal of Applied Mathematics,47(3), 2017, pp. 287-294.

[24] Opanuga, A. A., Okagbue, H. I. and Agboola, O. O. Irreversibility analysis of a radiative MHD poiseuille flow through porous medium with slip condition, Proceedings of the World Congress on Engineering 2017 Vol I WCE 2017, July 5-7, 2017, London, U.K.

[25] Zhou, J. K. Differential Transformation and its Applications for Electrical circuits. China: Huazhong University Press, 1986.

[26] Biaza, J. and Eslami, M. Differential transform method for Quadratic Riccati differential equation. International Journal of Nonlinear Science, 9(4), 2010, pp. 444-447.

[27] Agboola, O. O., Gbadeyan, J. A., Opanuga, A. A., Agarana, M. C., Bishop, S. A. and Oghonyon, J. G. Variational Iteration Method for Natural Frequencies of a Cantilever Beam with Special Attention to the Higher Modes, Proceedings of The World Congress on Engineering and Computer Science 2017, London, UK, July 5-7, 2017.

[28] Agboola, O. O., Opanuga, A. A. and J.A. Gbadeyan, Solution of third order ordinary differential equations using differential transform method, Global Journal of Pure and Applied Mathematics, 11(4), 2015, pp. 2511-2517.

[29] Opanuga, A. A., Edeki, S. O., Okagbue, H. I. and Akinlabi, G. O. A novel approach for solving quadratic Riccati differential equations. International Journal of Applied Engineering Research, 10 (11), 2015, pp. 29121-29126.

[30] Opanuga, A. A., Edeki, S. O., Okagbue, H. I. and Akinlabi, G. O. Numerical solution of two-point boundary value problems via differential transform method, Global Journal of Pure and Applied Mathematics, 11 (2), 2015, pp. 801-806.